J. Cosmet. Sci., **61,** 421–437 (November/December 2010)

Stable environmentally sensitive cationic hydrogels for controlled delivery applications

NAMITA DEO, S. RUETSCH, K.R. RAMAPRASAD, and Y. KAMATH, *TRI/Princeton, 601 Prospect Avenue, P. O. Box 625, Princeton, NJ 08542.*

Accepted for publication July 26, 2010.

Synopsis

New thermosensitive, cationic hydrogels were synthesized by the dispersion copolymerization of *N*-isopropylacrylamide (NIPAM) and (3-acrylamidopropyl)trimethylammonium chloride (AAPTAC). In the polymerization protocol, an amide-based comonomer, (3-acrylamidopropyl)trimethylammonium chloride, was reacted as a new alternative monomer for introducing positive charges into the thermosensitive hydrogel. The hydrogels were synthesized without making any pH adjustment in the aqueous medium. These hydrogel particles exhibited colloidal stability in the pH range of 1.5 to 11.0, while similar cationic hydrogels were reported to be unstable at pHs higher than 6. The stronger cationic character of the selected comonomer provided higher colloidal stability to the poly(NIPAM-co-AAPTAC) hydrogels. Furthermore, these hydrogels displayed sensitivity towards temperature, pH, and salt concentration. Interestingly, the particle size of hydrogels was found to be decreased significantly with an increase in temperature and salt concentration. In addition, using pyrene fluorescence spectroscopy, it was established that the hydrophobicity/hydrophilicity of the hydrogel particles was largely controlled by both pH and temperature. The thermosensitive hydrogels reported in this paper may be suitable for delivering different actives for cosmetic and medical applications. Although direct application of these hydrogel particles in cosmetics has not been shown at this stage, the methodology of making them and controlling their absorption and release properties as a function of temperature and pH has been demonstrated. Furthermore, these hydrogels may also have applications in scavenging organic and inorganic toxics.

INTRODUCTION

Environmentally responsive hydrogels have been subjects of great interest for the past few years due to their versatile applications. Such hydrogels are termed "intelligent" or "smart" since their properties enable them to react in a specific way to changes in the environment. Thermo-responsive synthetic hydrogels, exhibiting a lower critical solution temperature (LCST) in aqueous solution over a narrow temperature range, have received much attention recently. They swell and expand below the LCST but deswell and shrink above that temperature. The major cause for the LCST phenomenon is the entropy-driven hydrophobic interaction of polymer chains that have a delicate

Address all correspondence to Namita Deo at ndeo@triprinceton.com, nd157@yahoo.com

balance of hydrophilic and hydrophobic moieties in the structure. Among them, the most extensively studied thermosensitive polymer is poly-*N*-isopropylacrylamide (PNIPAM), which exhibits a lower critical solution temperature (LCST) of 34°C (1,2). Chemically cross-linked PNIPAM hydrogels reveal a drastic particle size decrease upon heating in aqueous solution. The responsive characteristics of these hydrogels have been modified further using both co-polymerization and advanced polymer architecture (3,4).

Cationically charged poly(NIPAM) hydrogels attracted significant attention particularly as carriers for affinity chromatography and diagnostic test applications (5–7). The phase transition behavior of monodisperse cationically charged poly(NIPAM) hydrogel particles was investigated by fluorescence spectroscopy (8). Poly(NIPAM) hydrogels with amino groups were used as carriers for the immobilization of oligodeoxyribonucleotides for the enhancement of diagnostic test sensitivity (9). Cationic poly(NIPAM) hydrogels and their magnetic forms were successfully tried as support materials for the specific extraction of nucleic acids (10,11). The adsorption of HIV-1 capsid p24 protein onto thermosensitive and cationic core shell poly(styrene)-poly(NIPAM) particles was investigated by Duracher *et al.* (12). The synthesis and colloidal properties of NIPAM-dimethylaminoethyl methacrylate copolymer hydrogels were investigated by Zha *et al.* (13–14) and by Zhang *et al.* (15). In the past few years, 4-vinylpridine, vinylimidazole, and *n*-vinylformamide were proposed as comonomers in the synthesis of NIPAM-based cationic hydrogels (16–25).

In the synthesis of poly(NIPAM)-based cationic hydrogels, mostly methacrylate-based comonomers (i.e., aminoethyl methacrylate or dimethylaminoethyl methacrylate) have been used to incorporate cationic groups into the structure of poly(NIPAM) particles (9–16). In this study, a thermosensitive cationic hydrogel was first synthesized by using an amide-based cationic comonomer, (3-acrylamidopropyl)trimethylammonium chloride. Responses of these hydrogels to various stimuli, such as temperature, pH, and salt and urea concentration, were explored using AFM, SEM, light-scattering, fluorescence, and UV-visible and FTIR spectrophotometric investigations.

For the delivery of a cosmetically active ingredient via encapsulation in a hydrogel nanoparticle, there are two basic requirements. One of these is a cationic charge that will help the particles to adsorb on the surface of hair, and the second requirement is the diffusion of the active out of the particle by changing the environmental conditions, such as an increase in temperature. For a rinse-off system, such as a shampoo or a conditioner, the particle size is critical. In a rinse-off situation the particles adsorbed on hair experience the force of adhesion between the particle and the hair surface and the viscous drag of the wash water flowing through the hair assembly in contact with the particles. Viscous drag is proportional to the surface area of the particle (hence the square of the particle diameter). It is very likely that the larger particles will be washed off the surface, leaving no residue. Therefore, it is imperative that the particle size be in the range of about 500 nm. This is based on the unpublished work done at TRI/Princeton on the deposition of anionic polystyrene particles on cationically modified hair surface.

When acrylamide derivatives are used, toxicity of the monomer becomes a question. Since the monomer is soluble in water, it can be washed away easily. This is the reason why acrylamide polymers are often used in water purification.

EXPERIMENTAL

MATERIALS

N-Isopropylacrylamide (NIPAM, 99%, Aldrich) was purified by recrystallization from a 60:40 toluene:hexane mixture. We employed (3-acrylamidopropyl)trimethylammonium chloride (AAPTAC, 75 wt%, Aldrich), *N,N*-methylenebisacrylamide (MBA, 99+%, Aldrich), sodium dodecyl sulfate (SDS, 98%, Aldrich), and ammonium persulfate (APS, 99%, Sigma) as received. The water used in the synthesis was of Millipore Milli-Q grade.

METHODS

Hydrogel preparation. Polymerization was conducted in a 250-ml three-necked flask equipped with a reflux condenser, a thermometer, and a nitrogen-bubbling tube. NIPAM (1.1316 g), SDS (1 g of 0.1M SDS), AAPTAC (0.1012 g) and MBA (0.075 g) were all dissolved in 100 ml of water. The solution was heated while being stirred to the polymerization temperature of 70°C and maintained at 70°C using a thermostated oil bath. Nitrogen was bubbled into the solution for 30 minutes to remove oxygen completely before the APS aqueous solution was added. An appropriate amount of APS was dissolved in 10 ml of water and injected to initiate the polymerization. The polymerizations were carried out for six hours under nitrogen atmosphere. After cooling, all hydrogels were purified by at least five cycles of ultracentrifugation (Beckman model L7-55, 45 min at 12000*g*), decantation, and redispersion in water. The hydrogels were lyophilized and stored at 4°C.

Fourier transform infrared analysis. FTIR spectra of hydrogels and all the monomers were determined using a Nicolet 560 FTIR spectrophotometer. At least 256 scans were obtained to achieve an adequate signal-to-noise ratio. The spectral resolution was 2 cm^{-1}. Spectroscopic grade KBr was dried under vacuum for 48 hours before use to make sure that all the water had been removed completely. One hundred milligrams of pre-dried KBr and 10 mg of each dried sample were mixed thoroughly using mortar and pestle. The KBr pellet was made using a pellet-making press. The attenuated total reflectance spectra of the KBr pellets were collected from 400 cm^{-1} to 4000 cm^{-1}.

Absorbance measurements. Absorbance measurements were made at different temperatures using a Shimadzu UV-240 spectrophotometer (cell length 5 cm). The hydrogel suspension was diluted to get an absorbance of approximately ≅0.25 at 500 nm at 20°C. Then the samples were equilibrated to the required temperature values by immersing the suspension in a water bath for 30 minutes.

The stability of the hydrogel was evaluated by using a spectrophotometric protocol. For this purpose, the absorbance of a diluted dispersion containing 0.1% (w/w) copolymer particles at different pHs was measured in the wavelength range of 300–700 nm. These measurements were conducted in the pH range of 4–10 by adjusting the pH with aqueous NaOH or HCl solution. The stability parameter, n, was calculated according to equation 1 by using the plots including the linear variation of absorbance with the wavelength, where A is the absorbance at a certain wavelength, λ:

$$n = \frac{-d \log A}{d \log \lambda} \quad (1)$$

The thermoresponsive behavior of the hydrogels was also monitored by a UV-visible spectrophotometer. The absorbance measurements were carried out at 500 nm under both heating and cooling conditions.

Zeta potential measurements. The zeta potential of hydrogel dispersion (solid content: 0.1%, w/w) was measured at different pH values at 25°C in a Zeta Sizer (Malvern Instruments, 3000 HSA, London, UK). The hydrogels were dispersed in 10^{-3}M KNO_3 solution to keep the electrolyte concentration constant. The pH was adjusted by the addition of 0.01 M Na(OH) or 0.01 M HCl. The zeta potential was calculated from the average electrophoretic mobility for ten particles per point. The average value of at least three measurements was taken at a given pH value.

Dynamic light-scattering measurements. The hydrodynamic particle diameters of hydrogels were determined both under heating and cooling conditions using dynamic light scattering (DLS) at a detector angle of 90°. A Lexel 95 ion laser operating at a wavelength of 488 nm and a power of 100 mW was used as the light source. Correlation data were analyzed using a BI-9000AT digital autocorrelator, version 6.1 (Brookhaven Instruments Corp.), and the CONTIN statistical method was used to calculate the particle size distributions. The hydrogels used in this study were highly monodisperse. Samples were prepared in thoroughly cleaned vials by suspending a small quantity of lyophilized hydrogels in filtered 10^{-3} M KCl. Sample pH values were adjusted using 0.1 M HCl and NaOH. The samples were temperature controlled to ± 1°C. Decalin, a refractive index matching liquid, was used to reduce light bending at the glass interfaces.

At least five replicate measurements were conducted for each sample; the experimental uncertainties represent the standard deviation of the replicate measurements. The samples were thermostated for at least 30 minutes to equilibrate the system.

From light-scattering measurements a ζ-average translational diffusion coefficient, D_0, was calculated (26). According to the Stokes-Einstein equation, the translation diffusion coefficient at zero concentration depends on the effective hydrodynamic sphere radius, R_h, which can be calculated from the equation for D_0 given below:

$$D_0 = \frac{k_B T}{6\pi\eta_0 R_h} \quad (2)$$

where k_B is the Boltzmann constant, T is the absolute temperature, and η_0 is the solvent viscosity (27). The system used was a BI-9000AT (Brookhaven Instrument Corp.), which allows DLS measurements at various scattering angles.

Atomic force microscopy (AFM). An atomic force microscope (AFM) (Digital Instrument Nanoscope (3A)) was used in contact mode to observe the topology of the hydrogel particles. Samples were prepared by coating the particles on previously cleaned glass surfaces at room temperature. The tips used for the experiments were silicon nitride tips.

SEM technique and sample preparation (SEM). A Hitachi S-4500 cold field emission scanning electron microscope (FESEM) was used for this study. Image acquisition was carried out at a low accelerating voltage, a long working distance, and a short scanning time to minimize beam damage to the substrate.

The various materials were stored and handled at an ambient temperature of 18.5°C to 19.5°C and ~50% RH prior to and during application to the hair fibers. Representative hydrogel particles were coated on the precleaned glass coverslips in different environmental conditions and then air-dried. The samples were mounted in parallel on double-sided tape onto SEM stubs. All samples were subsequently coated with approximately 60 Å of platinum for better conductivity and improved contrast, and were viewed at suitable magnifications to display the characteristic physical nature of the nano-particulate deposited on the glass coverslip surface in the best possible way.

Fluorescence measurements. Freeze-dried hydrogel particles were added to water-saturated pyrene solution at different pH levels and equilibrated for 12 hours. The pyrene fluorescence spectra were measured using a SPEX FluoroMax-2 spectrofluorometer. The excitation wavelength was 335 nm and the emission was monitored between 350 nm and 600 nm.

The ratio of the intensity of the third (I_3 at 383 nm) to the first (I_1 at 373 nm) fluorescence band of pyrene monomer (I_3/I_1) reflects the polarity experienced by the fluorescence probe (28–33). The peak around 480 nm is assigned to the excimer fluorescence of pyrene, and the intensity ratio of the excimer fluorescence (I_e at 480 nm) to the first (I_1 or I_m at 373 nm) is the measure of pyrene excimer formation.

RESULTS AND DISCUSSION

Thermosensitive cationic hydrogels have been prepared using a one-pot synthesis technique. The chemical structure of the hydrogel is illustrated in Figure 1. The chemical composition of the synthesized hydrogel was verified using FTIR measurements.

FTIR

Figure 1 shows typical FTIR spectra of both starting monomers and hydrogel particles. The IR spectrum of the polymer particles shows the characteristic absorption bands of cationic monomer (AAPTAC) at 3085 cm^{-1}, and 1646 cm^{-1}, the characteristic peak of NIPAM at 3290 cm^{-1}, and the characteristic peak of MBA at 1381 cm^{-1}. This confirms that the condition used for the synthesis of the thermosensitive cationic hydrogels is very effective in incorporating the comonomers into the structure.

AFM AND SEM MEASUREMENTS

Figure 2 illustrates the contact-mode AFM image of a glass surface covered with hydrogel particles. The image was obtained in ambient air. A clear and stable image could be obtained only when a relatively weak loading force was applied. When the loading force was

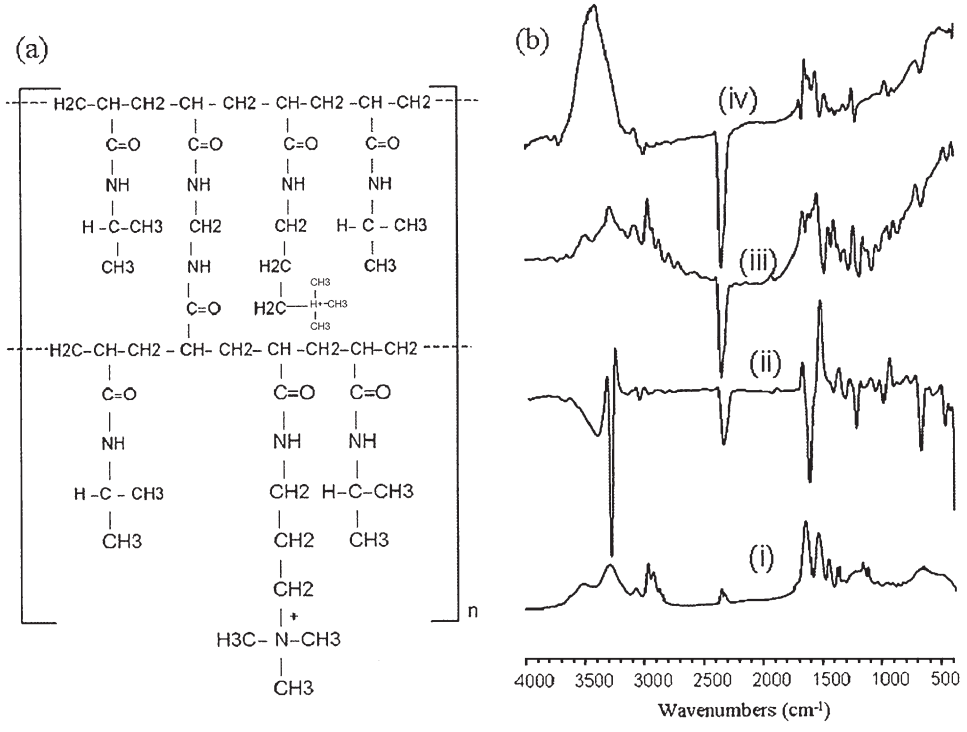

Figure 1. (a) Chemical structure of the hydrogel (b) FTIR spectra of (i) hydrogel, (ii) bis-acrylamide, (iii) acrylamide, and (iv) (3-acrylamidopropyl)trimethylammonium chloride.

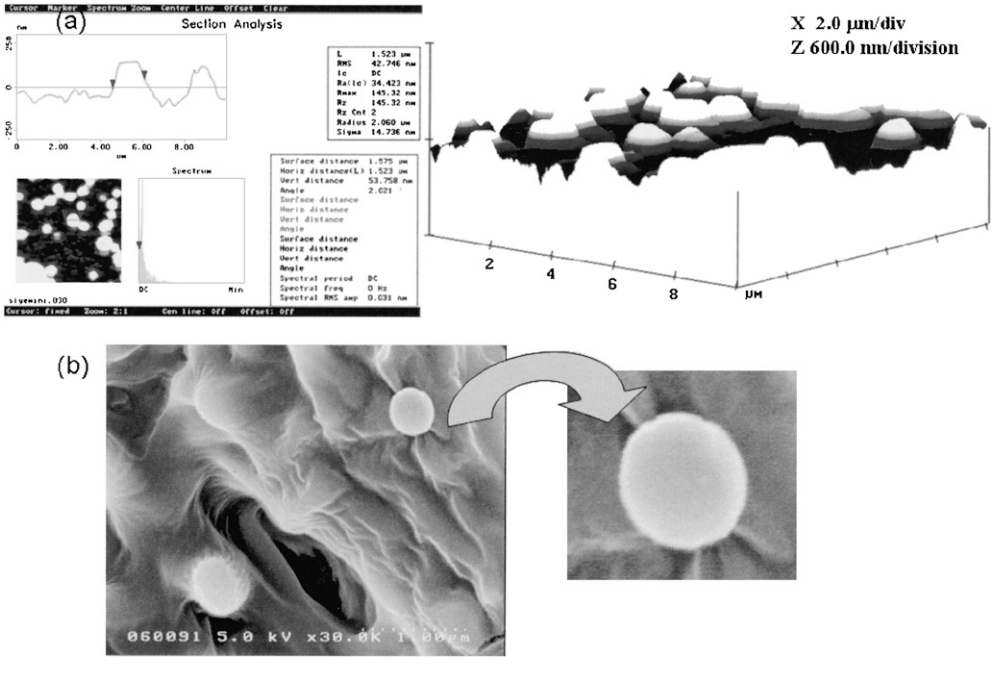

Figure 2. (a) AFM and (b) SEM images of hydrogel particles.

increased, the image showed an increasing number of horizontal lines (streaks), indicative of the mechanical sweeping out of hydrogel particles by the AFM tip. The result shows that a uniform hydrogel particle submonolayer can be formed on the glass surface and that the hydrogel–glass bonds provide strong enough binding for the particle to tolerate the contact-mode tip scanning. The measured width from the AFM topographic cross section is approximately 1.5 μ, substantially larger than the value determined from the SEM image (200 nm) shown in Figure 2. This change in particle diameter is attributed to the swollen state of hydrogels due to hydration.

Figure 3 shows the AFM and SEM micrographs of hydrogel particles taken directly from the preparation. The colloidal particles appear to have collapsed and there is material bridging the particles together. It is believed that the straight-chain copolymers that were unable to form the particles due to configurational restraints were coated on the hydrogel particles, thus acting as the bridging materials. These entangling materials were removed during the centrifugation and redispersion processes.

In Figure 4 the same hydrogel particles are shown after successive centrifugations and redispersions in distilled water. The particles are found to be monodisperse, with a diameter of about 1.7 μm. During the centrifugations and redispersion processes, the straight-chain copolymers, which were acting as the bridging elements and were responsible for making the solution viscous, were preferentially removed due to the differences in density. Furthermore, the unutilized monomers and indigenously formed salts were also separated during these processes. Therefore, the diameter of the hydrogel particles increased marginally due to encapsulation of a larger amount of water.

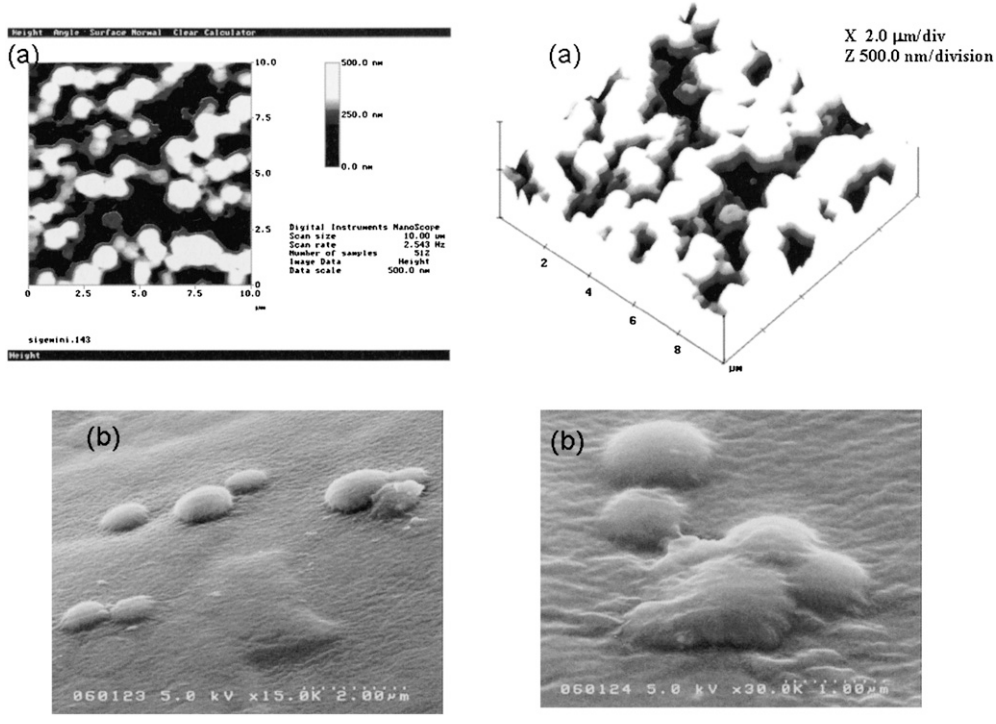

Figure 3. (a) AFM and (b) SEM images of hydrogels as synthesized.

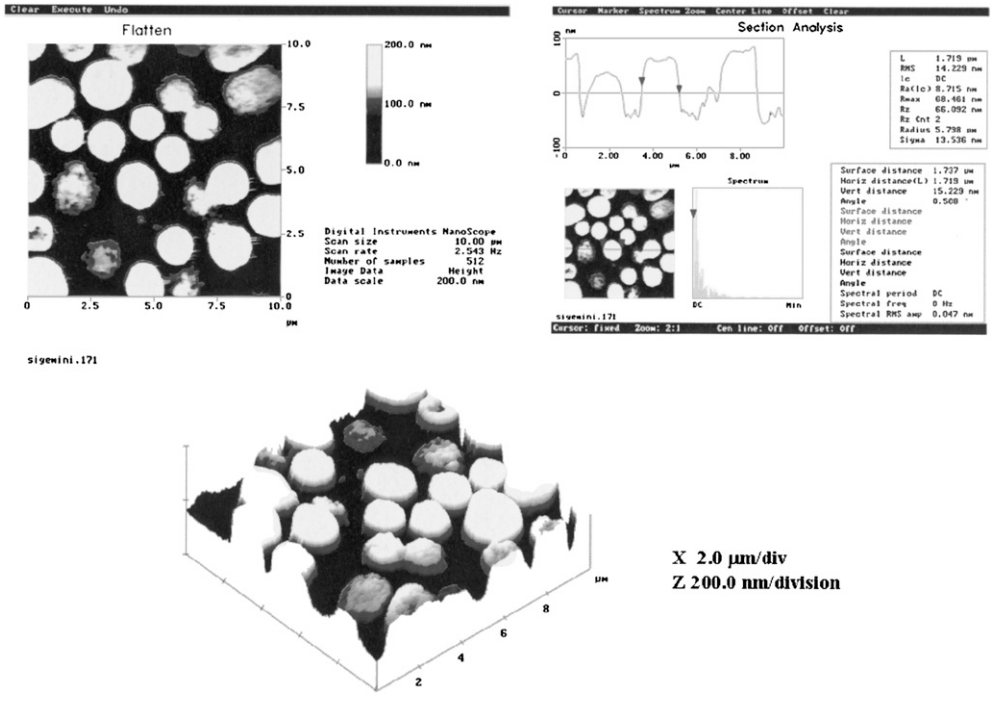

Figure 4. AFM images of hydrogels after five times successive centrifugations.

STABILITY PARAMETER

The variation of the stability parameter with pH is illustrated in Figure 5. As seen here, the hydrogel dispersion was very stable in the pH range studied. The stability of the hydrogels is attributed to the stronger electrostatic repulsion between positively charged units located on the copolymer particles.

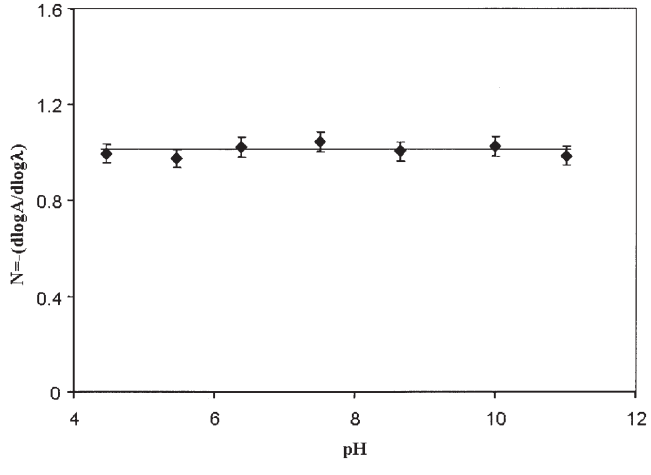

Figure 5. The variation of the stability parameter of hydrogels "n" with pH at 25°C.

ZETA POTENTIAL

Figure 6 shows the variation of the zeta potential as a function of pH. It was found that the zeta potential decreased when the pH increased above 7.0, which can be attributed to the partial neutralization of surface charges, in agreement with the previously reported results (34).

ABSORBANCE

Figure 7 represents the absorbance (light scattering) as a function of temperature. The amount of light scattered showed a dramatic increase when the temperature was raised above the LCST of poly(NIPAM). Therefore, it would appear that when the temperature was raised past the LCST of the polymer, the particles shrank, which resulted in an increase in the refractive index and in light scattering. It should be noted that the experiments in

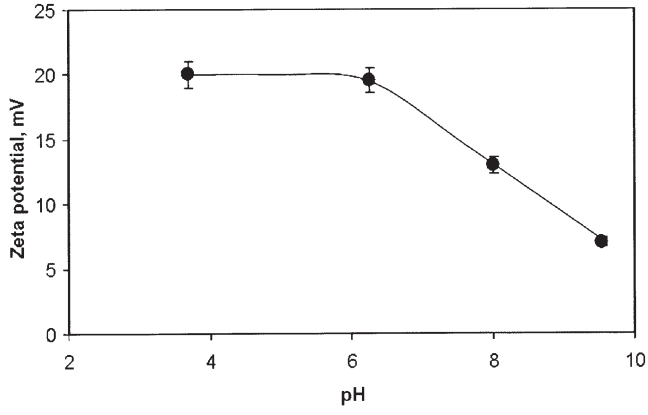

Figure 6. The variation of the zeta potential with pH.

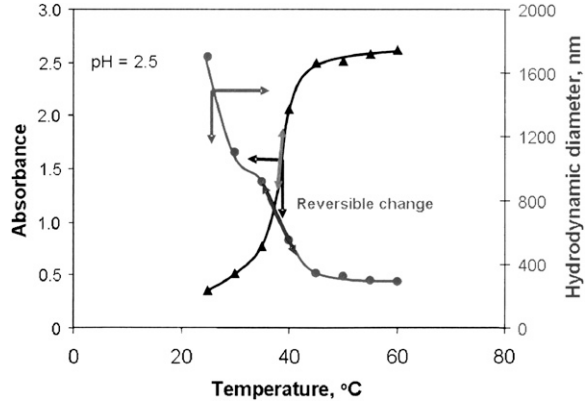

Figure 7. Change in optical density and hydrodynamic diameter of cationically modified hydrogels as a function of temperature.

Figure 7 were conducted in the absence of any added electrolyte and that the particles remained colloidally stable over the temperature range shown here. Indeed, the absorbance curves were reversible. To further verify the reversibility of the swelling and deswelling behavior of hydrogel particles, the hydrogel suspension as obtained was thermally cycled between 25°C and 40°C. Figure 8 shows the reversible swelling and deswelling of hydrogel particles when thermally cycled between 25°C and 40°C. It can be noticed that hydrogel particles exhibit similar values of effective diameter at each temperature even after several thermal cycles, suggesting that the hydrogel particles are capable of maintaining structural integrity during the repeated swelling-deswelling cycles. Furthermore, it was found that the kinetics of swelling and deswelling of hydrogels in response to thermal stimuli were very fast.

The effect of temperature on the hydration/dehydration behavior of hydrogel particles was further verified using AFM and is illustrated in Figure 9. It is clearly evident from the figure that if the particles are deposited on the glass surface at a temperature above the LCST, the size of the hydrogel particles decreases markedly—for example, from 1.6 μ to around 680 nm, which is in agreement with the light-scattering and absorbance results.

The degree of absorbance change was found to be relatively less affected with an increase in pH (Figure 10). AAPTAC, a quaternized ammonium salt, strongly dissociates in aqueous solution, probably rendering the degree of hydrogel swelling relatively insensitive to pH.

The continuous changes in water content in the hydrogels as a function of temperature can be explained in the light of different proposed models. According to Heskins and Guillet (35), PNIPAM particles behave as flexible coils that undergo extensive intermolecular association near the LCST. This model was based on an analysis of sedimentation and viscosity measurements at ambient temperature of an unfractionated PNIPAM sample and on the temperature dependence of these properties. However, whether these intermolecular associations are also prevalent at ambient temperature has not been established

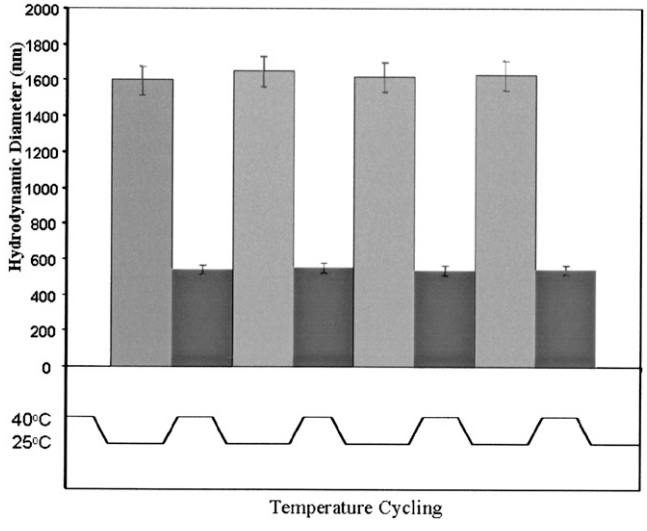

Figure 8. Reversible swelling and deswelling behavior of hydrogel particles when the temperature was cycled between 20°C and 40°C.

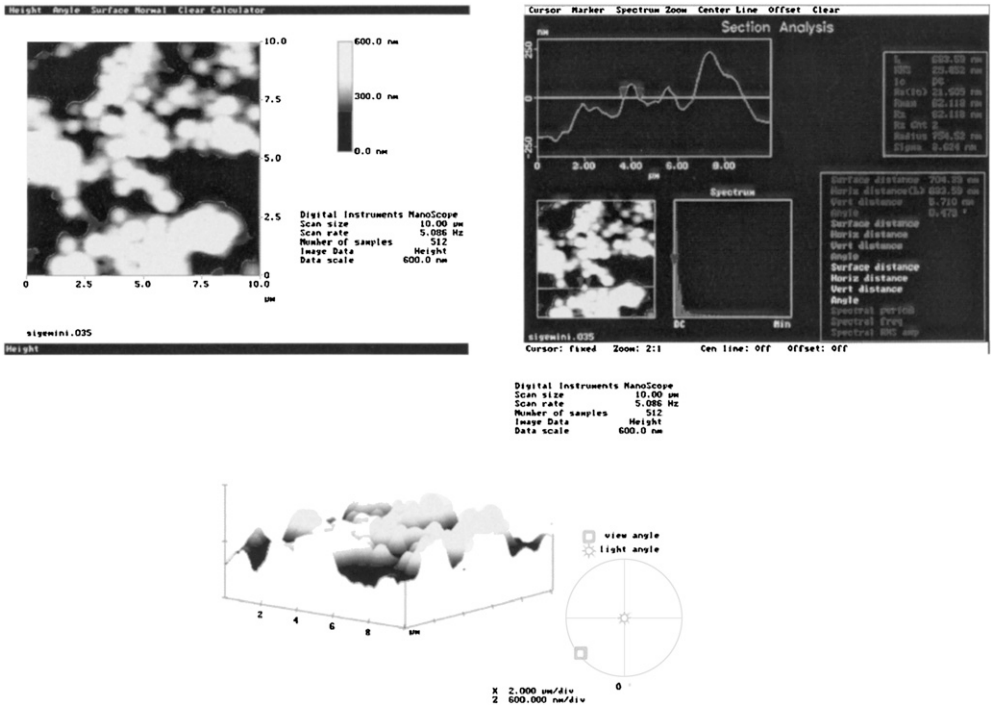

Figure 9. AFM images of hydrogels at 40°C.

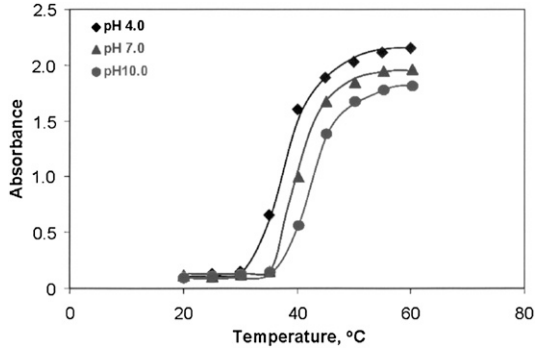

Figure 10. Absorbance of hydrogel suspensions as a function of temperature at different pH values (λmax = 500 nm).

unambiguously, but it may be implied from circumstantial evidence, such as solution aging effects on viscosity and osmometry measurements (36). Water is a special solvent for PNIPAM in view of the large difference between the Hildebrand solubility parameters of water (δ23.4) (36). and of PNIPAM (δ 13–14 (38), 11 (39)). Normally a polymer is soluble in liquids, having solubility parameters only within the range of $\delta \pm 3$.

From a thermodynamic point of view, the formation of hydrogen bonds between water molecules and the amide groups of the polymer contributes favorably to the free energy of mixing ($\Delta G_M < 0$), but unfavorably to the entropy of mixing (ΔS_M). Hydrogen bonding

between the water and the polymer triggers the formation of a layer of highly organized water molecules around the polymer, which decreases the entropy of the system. Association between polymeric chains via hydrophobic interactions between the alkyl substitutents can occur as well. These interactions become significant as the temperature of the solution is increased and the bound water is released. Then the relative values of the thermodynamic functions change: the entropic term becomes dominant, resulting in a positive free energy of mixing (ΔG_M). This favors a two-phase system. Therefore, the absorbance of the hydrogel suspension increases significantly after the LCST has been reached and the encapsulated water has been squeezed out.

FLUORESCENCE

The stimuli-responsive behavior of the hydrogel particles were also examined using pyrene fluorescence. Pyrene has a much lower solubility in water (about 10^{-7} mol/l) than hydrocarbons (0.075 mol/l). It migrates from the water phase into hydrophobic regions once it is formed in aqueous solution, with remarkable photophysical changes (40,42). The hydrophobicity/hydrophilicity of the hydrogels at different pH values as a function of temperature can be assessed by examining the intensity ratio of the third/first peak (I_3/I_1) of the pyrene fluorescence emission spectrum. The temperature effects on the shape of hydrogels were also determined by plotting the intensity ratio of the pyrene excimer peak/pyrene monomer peak (I_e/I_m) as a function of temperature at different pH values. The samples were prepared by adjusting the pH of the hydrogel suspension to different values, and then pyrene was added to the pH-preadjusted hydrogel suspension.

The variation of I_3/I_1 with temperature at different pH values is illustrated in Figure 11. An increase in I_3/I_1 with an increase in temperature was detected at all three pH values. Below the LCST, the hydrogels are very hydrophilic, as the hydrogels are fully hydrated with a large amount of water. Therefore, the encapsulated pyrene molecules experienced a

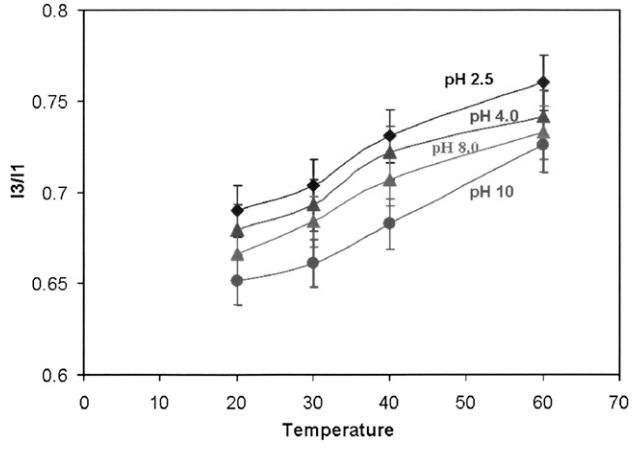

Figure 11. I_3/I_1 ratios of pyrene fluorescence of hydrogels as a function of temperature at different pH values.

hydrophilic environment. With an increase in temperature above the LCST of the polymer, the particles are dehydrated, resulting in an increase in the hydrophobic environment in the core. Hence the I_3/I_1, which is the measure of the polarity of the environment, increases significantly once the pyrene molecules sense the hydrophobic environment of the dehydrated hydrogel core. Similar behavior was observed at all the pH levels. Also, in this figure, the magnitude of I_3/I_1 difference between the lower and upper values should be considered as an indicator for the thermosensitivity of hydrogel dispersion. The lower I_3/I_1 values observed at the low temperature range correspond to the completely hydrated hydrogel dispersion, whereas higher values at high temperature give the I_3/I_1 values of shrunken particles. Furthermore, a consistent decrease in I_3/I_1 with an increase in pH was detected over the entire temperature range used in this study, suggesting pH dependence of the hydrophobic/hydrophilic behavior of the hydrogels.

When a solution of PNIPAM/Py in water is heated from 20°C to 60°C, several events seem to be occurring, as illustrated in Figure 12. The ratio I_e/I_m increases slightly to reach a maximum value. Then it decreases sharply to reach a limiting value. These changes are reversible: upon slow cooling of the solution, the ratio I_e/I_m increases and returns to its initial value.

EFFECTS OF SALT ON THE SWELLING BEHAVIOR OF HYDROGELS

The volume phase transition behavior of hydrogels in the presence and the absence of salt was characterized using an atomic force microscope and is illustrated in Figure 13. It is evident from the figure that in the presence of 0.1M NaCl, at pH 7.0, the hydrogels deswell significantly. For example, the cubic ratio of the particle sizes at 0 and 0.1M NaCl $(d0/d0.1)^3$ was 15.08. The observed phenomenon can be clearly explained using simple physical evidence.

At low ionic strength or in the absence of any salt, the concentration of bound charges (and accompanying co-ions) within the gels exceeds the concentration of salt in the external

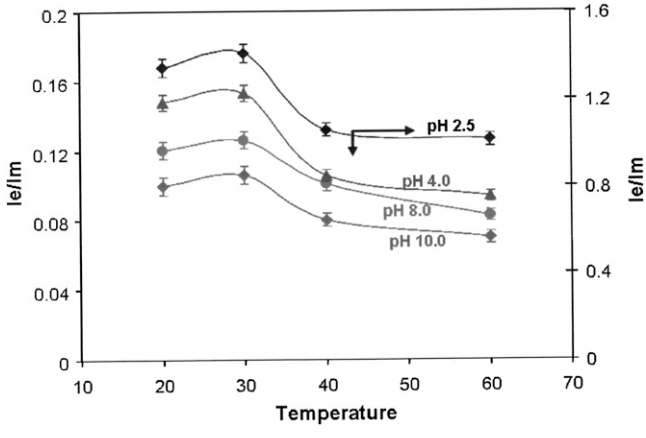

Figure 12. The ratio of excimer to monomer intensities (I_e/I_m) of pyrene in hydrogel suspensions as a function of temperature at different pH values.

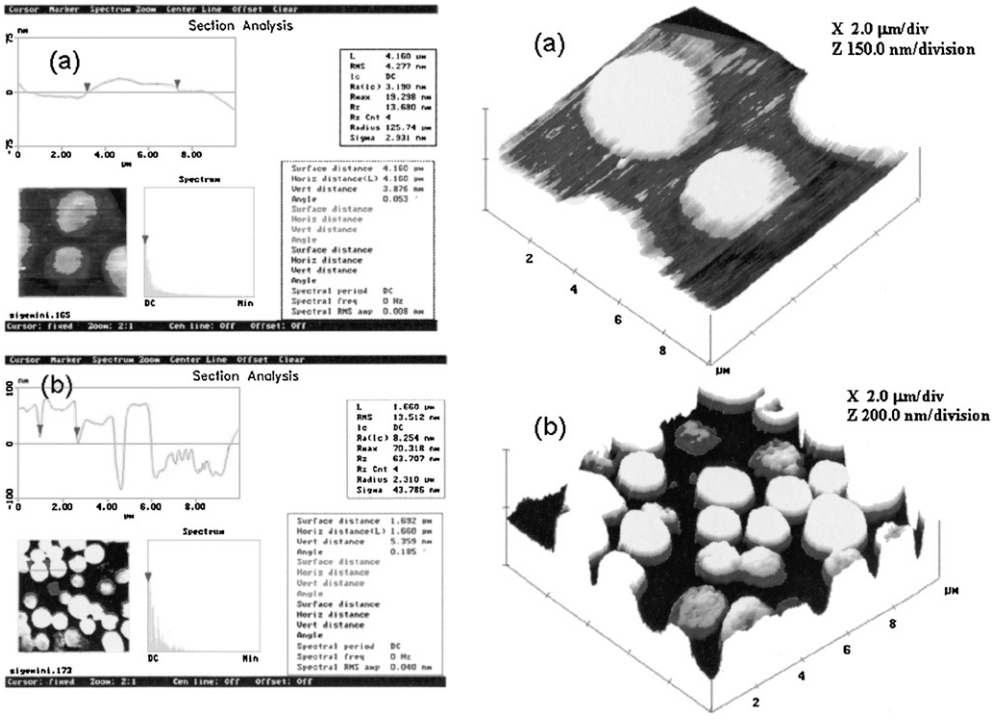

Figure 13. AFM images of hydrogels in the (a) absence and (b) presence of 0.1 M NaCl.

solution; therefore, a large ion-swelling pressure causes the hydrogels to expand, thereby lowering the concentration of co-ions within the gels. As the external salt concentration rises, the difference between the internal and external ion concentrations decreases and the gel deswells. The gel continues to deswell with rising external salt concentration until the mobile ion concentrations within and surrounding the gel are approximately equal. Furthermore, the swelling behavior of the hydrogels in Figure 13 can also be explained on the basis of repulsions between fixed charge groups on the hydrogel particles. At low ionic strength, (large Debye lengths), repulsions are long-range and the gel expands to minimize the repulsive free energy; as ionic strength rises (smaller Debye lengths), repulsions are shielded and the gel deswells. Therefore, in the presence of 0.1 M NaCl, the particle size decreases from 4.1 µm to 1.6 µm; this is clearly demonstrated using atomic force microscopy. Furthermore, it is clearly shown using both AFM and SEM (Figure 14) that if the hydrogel samples are allowed to dry in the presence of an excess amount of NaCl, the particles seem to lose their spherical shape, due to nonuniform dehydration.

EFFECT OF UREA ON THE TEMPERATURE-INDUCED VOLUME TRANSITION

Urea has been frequently employed in the biochemical field as a means to identify hydrogen bonds, since it is generally believed that urea can break up intra- or intermolecular hydrogen bonding of proteins/polymers in aqueous systems. Therefore, we studied

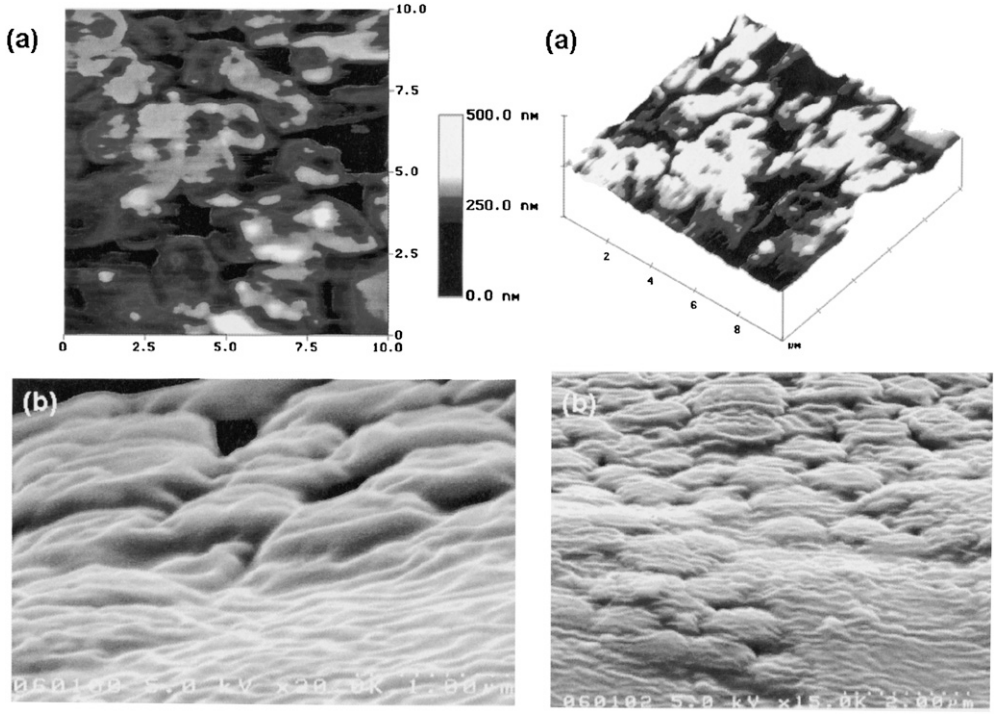

Figure 14. (a) AFM and (b) SEM images of hydrogel particles in the presence of an excess amount of NaCl.

the effects of urea to explore the mechanisms of temperature dependence of hydrogel swelling at different pH values (Figure 15) and found that urea reduces the temperature effect significantly on the phase separation of hydrogel suspensions at pH 4.0 and pH 10.0. On the other hand, at pH 7.0, a small reduction in absorbance was observed after the LCST even in the presence of 20% urea. Compared to higher pH levels, the effect of urea is more predominant at pH 4.0 due to the presence of a maximum number of positive charges and hence maximum hydrogen bonding. Furthermore, it has been seen that the effects of urea in the phase separation of a hydrogel suspension is irreversible in nature. Even after five days of dialysis against distilled water, the absorbance curve did not return to its original position (Figure 15a). These results confirm that intra/intermolecular hydrogen bonding plays an important role during the hydration and dehydration process of hydrogels.

Molecular level sensitivity towards different stimuli makes these hydrogels potential candidates for different delivery and toxic scavenging applications. Furthermore, it will be possible to tailor these hydrogels further to meet the need of specific applications by the proper selection of monomers.

CONCLUSIONS

In this study, multi-sensitive NIPAM-based uniform hydrogel particles were synthesized by using a relatively new amide-type cationic monomer. The obtained hydrogel dispersion

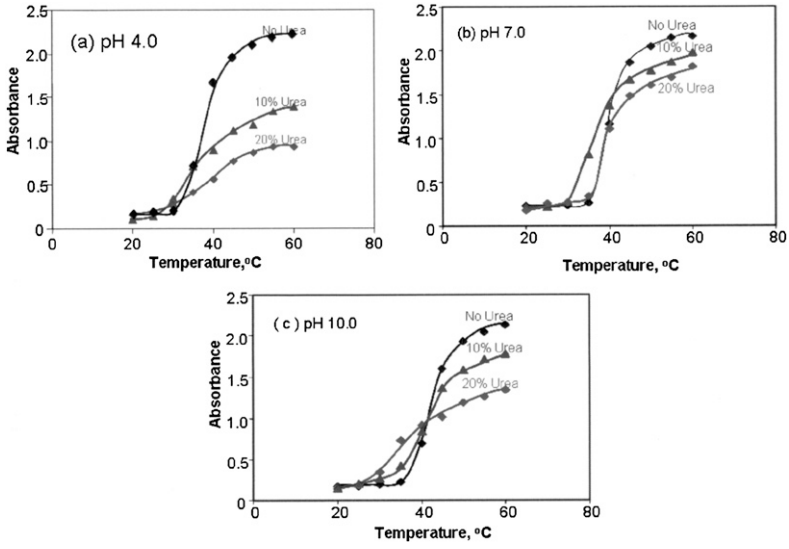

Figure 15. Change in absorbance as a function of temperature at (a) pH 4.0, (b) pH 7.0, and (c) pH 10.0.

exhibited colloidal stability in a wide pH range, comparable to that of similar cationic hydrogels. The hydrogel particles showed a very sharp volume transition over a temperature range of 25°C–40°C and a reversible swelling and deswelling behavior when the temperature was cycled between 20°C and 40°C. Fluorescence spectroscopy revealed the dispersion's pH-dependent hydrophobic/hydrophilic behavior. It was also found that the ionic strength of the hydrogel suspension should be kept lower than 0.1 M to observe a strong effect on hydrogel swelling.

Incorporation of temperature, pH, and ionic-strength-sensitive monomers in a single network provides flexibility for controlling swelling behavior by controlling related variables. Hence, by the proper selection of monomers, it will be possible to tailor a temperature-sensitive hydrogel to meet specific delivery or scavenging applications.

ACKNOWLEDGMENT

We are thankful to Prof. P. Somasundaran, Department of Earth and Environmental Engineering, Columbia University, New York, for allowing us to use AFM, light-scattering, and fluorescence spectrometry equipment.

REFERENCES

(1) R. H. Pelton and P. Chibante, *Colloids Surf.,* **20,** 247–256 (1986).
(2) R. Pelton, *Adv. Colloid Interface Sci.,* **85,** 1–33 (2000).
(3) C. D. Jones and L. A. Lyon, *Macromolecules,* **33,** 8301–8306 (2000).
(4) D. Gan, and L. A. Lyon, *J. Am. Chem Soc.,* **123,** 7511–7517 (2001).
(5) T. Tanuguchi, D. Duracher, T. Delair, A. Elaissari, and C. Pichot, *Colloids Surf. B,* **29,** 53 (2003).
(6) S. Rossi, C. Lorenzo-Ferreira, J. Battistoni, A. Elaissari, C. Pichot, and T. Delair, *Colloid Polym. Sci.,* **282,** 215 (2004).

(7) D. Duracher, F. Sauzedde, A. Elaissari, A. Perin, and C. Pichot, *Colloid Polym. Sci.,* **276,** 219 (1998).
(8) E. M. S. Castanheira, J. M. G. Martinho, D. Duracher, M. T. Charreyre, A. Elaissari, and C. Pichot, *Langmuir,* **15,** 6712 (1999).
(9) T. Delair, F. Meunier, A. Elaissari, M. H. Charles, and C. Pichot, *Colloid Surf. A,* **153,** 341 (1999).
(10) A. Elaissari, L. Holt, F. Meunier, C. Voisset, C. Pichot, B. Madrand, and C. Mabilat, *J. Biomater. Sci. Polym.,* **E10,** 403 (1999).
(11) A. Elaissari, M. Rodrigue, F. Meunier, and C. Herve, *J. Magnet. Mag. Mater,* **225,** 27 (2001).
(12) D. Duracher, A. Elaissari, F. Mallet, and C. Pichot, *Langmuir,* **16,** 9002 (2000).
(13) L. Zha, J. Hu, C. Wang, S. Fu, A. Elaissari, and Y. Zhang, *Colloid Polym. Sci,* **280,** 1 (2002).
(14) L. S. Zha, J. H. Hu, C. C. Wang, S. K. Fu, and M. F. Luo, *Colloid Polym. Sci.,* **280,** 1116 (2002).
(15) Y. Zhang, L. S. Zha, and S. K. Fu, *J. Appl. Polym. Sci.,* **92,** 839 (2004).
(16) V. T. Pinkrah, M. J. Snowden, J. C. Mitchell, J. Seidel, B. Z. Chowdhry, and G. R. Fern, *Langmuir,* **19,** 585 (2003).
(17) R. J. Hall, V. T. Pinkrah, B. Z. Chowdhry, and M. J. Snowden, *Colloids Surf. A,* **233,** 25 (2004).
(18) X. Li, J. Zuo, Y. L. Guo, and X. H. Yuan, *Macromolecules,* **37,** 10042 (2004).
(19) J. Seidel, V. T. Pinkrah, J. C. Mitchell, B. Z. Chowdhry, and M. J. Snowden, *Thermochim. Acta,* **414,** 47 (2004).
(20) S. Takata, M. Shibayama, R. Sasabe, and H. Kawaguchi, *Polymer,* **44,** 495 (2003).
(21) S. Ito, K. Ogawa, H. Suzuki, B. Wang, R. Yoshida, and E. Kokufuta, *Langmuir,* **15,** 4289 (1999).
(22) J. J. Xu A. B. Timmons, and R. Pelton, *Colloid Polym. Sci.,* **282,** 256 (2004).
(23) J. J. Xu and R. Pelton, *J. Colloid Interface Sci.,* **276,** 113 (2004).
(24) D. Kuckling and S. Wohlrab, *Polymer*, **43,** 1533 (2002).
(25) D. Kuckling, C. D. Vo, and S. E. Wohlrab, *Langmuir*, **18,** 4263 (2002).
(26) B. J. Berne and R. Pecora, *Dynamic Light Scattering (*Wiley-Interscience, New York, 1976).
(27) C. E. Ioan, T. Aberle, and W. Burchard, *Macromolecules* **34,** 326 (2001).
(28) D. C. Dong and M. A. Winnik, *Can J. Chem*. **62,** 2560 (1984).
(29) K. Kalyanasundaram, *Photophysics of Microheterogenous System* (Academic Press, New York, 1988).
(30) P. Chandar, P. Somasundaran, and N. J. Turro, *J. Colloid Interface Sci*. **117,** 31 (1987)
(31) J. K. Thomas, *The Chemistry of Excitation at Interfaces,* ACS Monograph 181 (American Chemical Society, Washington, DC, 1984).
(32) K. Kalyanasundaram and J. K. Thomas, *J. Am. Chem. Soc.* **99,** 2039 (1977).
(33) F. M. Winnik and S. T. A. Regismond, *Colloids Surf*. A, **118,** 1 (1996).
(34) L. S. Zha, J. H. Hu, C. C. Wang, and S. K. Fu, *Colloid Polym. Sci.,* **280,** 1116 (2002).
(35) M. Heskins and J. E. J. Guillet, *Macromol. Sci. Chem.,* 1441 (1968).
(36) M. P. Breton, PhD. Thesis, University of Toronto, Toronto, Canada, 1980.
(37) H. Burrell, in *Polymer Handbook,* 2nd Ed., J. Brandrup and E.H. Immergut, Eds. (John Wiley & Sons, New York, 1975), p. IV337.
(38) E. P. Abel and W. A. Bowman, *U.S. Patent 4,* 504, 569 (1985).
(39) H. J. Ahmad, *Macromol. Sci. Chem.,* **A17,** 588 (1982).
(40) M. Li, M. Jiang, and C. Wu, *Langmuir,* **16,** 9205 (2000).
(41) K. Kogej, J. Skerjanc, *Langmuir,* **15,** 4251 (1999).
(42) D. Y. Chu and J. K. Thomas, *Macromolecules,* **20,** 2133 (1987).